Dynamical Behaviors of Multicellular Chopper

Philippe Djondiné, Malek Ghanes, Jean-Pierre Barbot, Bernard Essimbi

Dynamical Behaviors of Multicellular Chopper

Philippe Djondiné[1, 2], Malek Ghanes[1], Jean-Pierre Barbot[1, 3] and Bernard Essimbi[2]

1. ECS-Lab (Laboratoire d'Electronique et Commande des Système) EA3649, ENSEA (Ecole Nationale Supérieure de l'Electronique et de ses Applications) Cergy Cedex, Cergy-Pontoise 95014, France

2. Department of Physics, Electronic Laboratory,Tthe University of Yaoundé I, BP 812, Cameroon

3. EPI Non-A INRIA (Equipe Projet INRIA Non-Asymptotic Estimation for Online Systems)

Abstract: In this paper, the behavior analysis of two cells chopper connected to a nonlinear load is reported. Thus, this is done in order to highlight the way to chaos. Furthermore, throughout the study of these dynamical behaviors of this complex switched system some basic dynamical properties, such as Poincaré section, first return map, bifurcation diagram, power spectrum, and strange attractor are investigated. The system examined in Matlab-Simulink. Analyses of simulation results show that this system has complex dynamics with some interesting characteristics.

Key words: Chaos, multicellular chopper, dynamical properties, chaotic attractor.

1. Introduction

Multicellular [1] converters have grown from an attractive theoretical concept to industrial applications, especially for using in higher power applications [1-6], and they are well suited to packaging of renewable energy sources. Indeed, due to their modular structure, they can be combined easily [5]. In recent decades, it was discovered that most of static converters were the seat of unknown nonlinear phenomena in power electronics [7-11]. It is, for example, It is for example the case of multicellular choppers that can exhibit unusual behaviors and sometimes chaotic behaviors Obviously, this may generate dramatical consequences (such as the 1 Megawatt multicellular chopper [12]). However, the usually averaged models do not allow to predict nonlinear phenomena encountered. By nature, these models obscure the essential nonlinearities [13]. To analyses these strange behaviors, it is necessary to use a nonlinear hybrid dynamical model [14, 15].

There have been many methods for detecting chaos from order [16]. They include routes to chaos with phase portraits, first return map, Poincaré sections, Lyapunov exponents [17], fast Lyapunov indicators [18], SAI (smaller alignment index) [19] and its generalized alignment index [20], bifurcations, power spectra [21], frequency analysis [22], 0-1 test [23], geometrical criteria [24, 25], and fractal basin boundaries [26], etc.. Each of them has its advantages and drawbacks in classifying the attractors.

The main purpose of the present paper is to use numerical approaches to study the dynamical properties of two-cells chopper connected to nonlinear load.

The rest of this paper is organized as follows. Section 2: the two-cells chopper connecting to a particularly nonlinear load modeling and analysising of a switching cell are presented. Basic dynamical properties of the chaotic system are also investigated in Section 3. Finally, chaotic behavior and simulation results are presented in Section 4.

Corresponding author: Philippe Djondiné, Ph.D. candidate, research field: dynamical properties analysis of power electronics converters. E-mail: pdjondine@yahoo.fr.

2. Multicellular Chopper Modeling

The multicellular converters (Fig. 1) are built starting from an association of a certain number of cells. At the output, one obtains (p + 1) levels (0, E/p, …, (p - 1)E/p, E). This association in series allows the output source to evolve on (p + 1) possible levels. As the orders of the switches of the cells of commutation are independent, one obtains 2^p possible combinations [27-31]. Thus, it is necessary to ensure an equilibrated distribution of the voltage of the floating condensers. Under these conditions, one obtains the following property:

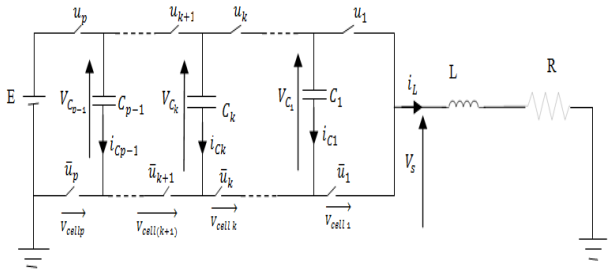

Fig. 1 P–cells chopper connected to RL load.

The converter has (p - 1) floating voltages sources and the voltage of the capacity of index k is $k = E/p$. The control signal associated with each commutation cell is noted as u_i, where i_L represents the number of cells of the topology. This signal will be equal to 1 when the upper switch of the cell is conducting and 0 when the lower switch of the cell is conducting.

Note that the chopper, which has a purely dissipative load, cannot generate a chaotic behavior. Nevertheless, it is well known from Ref. [5] that power converter, when it is connected to nonlinear load may have a chaotic behavior. The chopper modeling is:

$$\begin{cases} \dfrac{dV_{c1}}{dt} = \dfrac{u_2 - u_1}{C_1} i_L \\ \dfrac{dV_{c2}}{dt} = \dfrac{u_3 - u_2}{C_2} i_L \\ \quad \vdots \\ \dfrac{dV_{cp-1}}{dt} = \dfrac{u_p - u_{p-1}}{C_{p-1}} i_L \\ \dfrac{di_L}{dt} = \dfrac{u_2 - u_1}{L} V_{C1} + \cdots + \dfrac{u_p - u_{p-1}}{L} V_{cp-1} + \dfrac{u_p}{L} E - \dfrac{R}{L} i_L \end{cases} \quad (1)$$

For this model the load current i_L and the floating voltages V_{Ck} are used as space variables

To simplify the study and the notations, we will study the overlapping operation of a converter with two-cells (Fig. 2). Its function is to supply a passive load (RL) in series with another nonlinear load

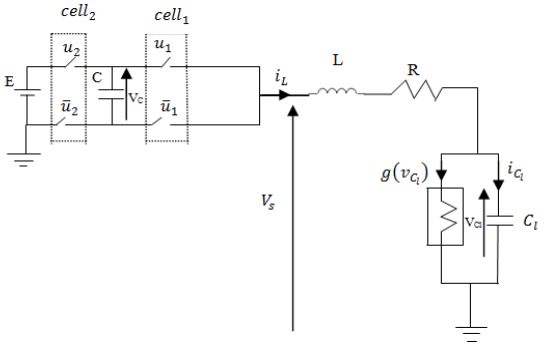

Fig. 2 Two-cells chopper connected to a nonlinear load.

Connected in parallel with a capacitor [13]. Four operating modes are then possible as shown in Fig. 3. Note that the floating source takes part in the evolution of the dynamics of the system only to the third and fourth mode. In the third mode, the capacity discharges and charge during the fourth mode. Thus, if these two modes last same time with a constant charging current, then the average power transmitted by this floating source over one period of commutation is null. We also notice that these two modes make it possible to obtain by commuting the additional level $E/2$ on the output voltage V_s.

As the switches of each cell are regarded as ideals, their behavior can be modeled by a discrete state taking of the values 0 (on) or 1 (off). In practice, some of these states never will be visited for reasons of safety measures or following the strategy of order adopted or because of the structure of the converter him finally to even or comply with the rule of adjacency. The transitions are not necessarily controlled.

The system model can be represented by three differential equations giving its state space.

$$\begin{cases} L\dfrac{di_L}{dt} = (u_2 - u_1)v_c - v_{cl} - R\cdot i_L + u_2\cdot E \\ C\dfrac{dv_c}{dt} = (u_2 - u_1)i_L \\ C_l\dfrac{dv_{cl}}{dt} = i_L - g(v_{cl}) \end{cases} \quad (2)$$

where,

$$g(v_{cl}) = G_b v_{cl} + \frac{1}{2}(G_a - G_b)(|v_{cl}+1| - |v_{cl}-1|)$$

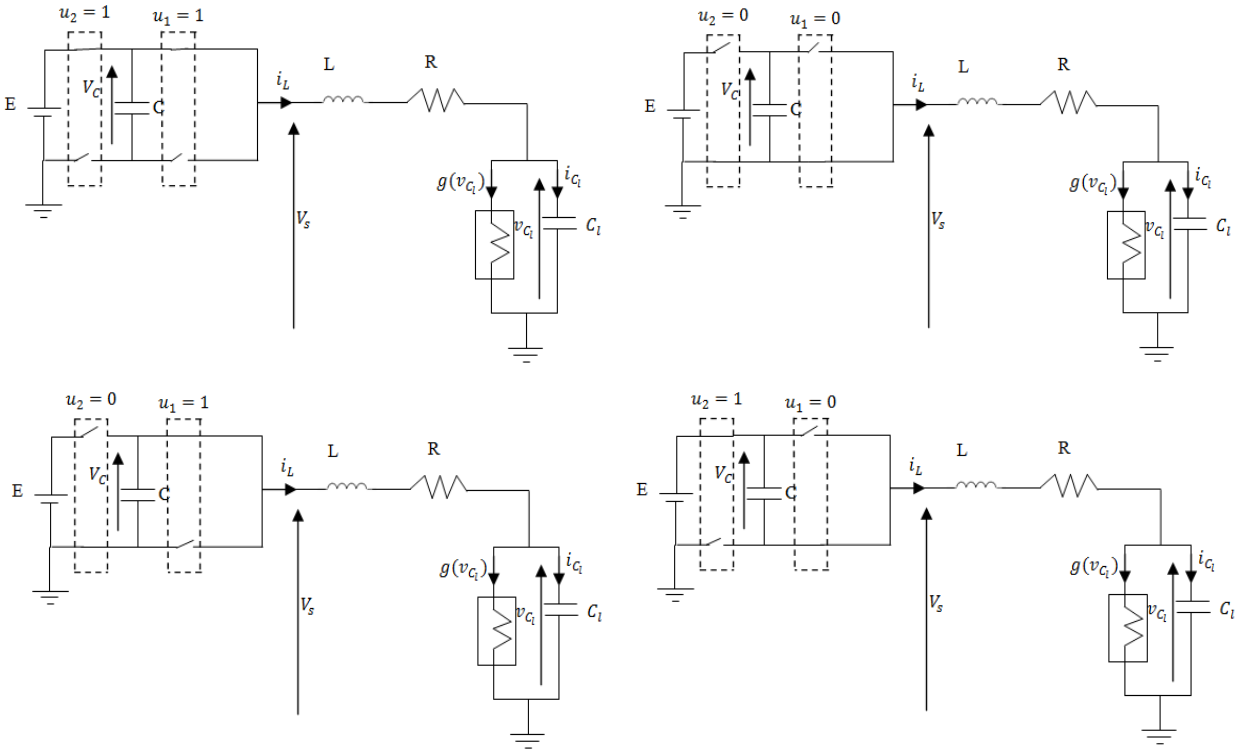

Fig. 3 Switching cell and its configurations.

which is the mathematical representation of the characteristic curve of nonlinear load. The slopes of the inner and outer regions are G_a and G_b. The parameters of the circuit elements are fixed as C = 0.1 μF, C_l = 40 μF, L = 50 mH, R = 10 Ω, E = 100 V.

3. Dynamical Properties

For the power converters, many methods like phase portrait, bifurcation diagram, and time-domain waveform can be used to analyze the nonlinear phenomenon in the system. In this work, the bifurcation diagrams and Poincaré sections are drawn based on the discrete iterated mapping model. Time-domain waveform, phase portrait, and power spectrum are obtained by building simulation module in Matlab/Simulink, which is analyzed from literature results.

Rescaling Eq. (2) as $v_C = x_2Bp$, $V_{Cl} = x_3Bp$, $i_L = x_1GBp$, $G = 1/R$, $t = (C/G)\tau$ (V_C denote the voltage across C, V_{Cl} denote the voltage across C_l, G denote the reactance) and then redefining τ as t the following set of normalized equations are obtained:

$$\begin{cases} \dot{x}_1 = \beta(-\gamma x_1 + \varepsilon x_2 - x_3) + \alpha E \\ \dot{x}_2 = \varepsilon x_1 \\ \dot{x}_3 = p(x_1 - g(x_3)) \end{cases} \quad (3)$$

where

$\varepsilon = u_2 - u_1$, $p = c / c_l$, $\beta = c / LG^2$, $\gamma = RG$, $\alpha = \beta E / B_p$.

Obviously,

$$g(x_3) = bx_3 + 0.5(a-b)[|x_3+1| - |x_3-1|]$$

or

$$g(x_3)=\begin{cases} bx_3+a-b, x_3>1 \\ ax_3, |x_3|\le 1 \\ bx_3-a+b, x_3<-1 \end{cases} \quad (4)$$

here, $a = G_a / G$, $b = G_b / G$.

Now the dynamics of Eq. (3) depends on the parameters ε, p, β, γ, a, b and α. The circuit parameters used are then rescaled as: $p = 25\times10^{-4}$, $\beta = 2\times10^{-4}$, $\alpha = 2\times10^{-2}$, a = -15, b = 5, γ = 1.

3.1 Symmetry and Invariance

We can see the invariance of the system under the coordinate transformation $(x_1, x_2, x_3)\rightarrow(x_1, -x_2, x_3)$. Also note that, in the x_3 versus x_2 plane there is symmetry around the nominal value of the voltage of the floating capacitor that is 50V. This symmetry is shown in Fig. 3.

3.2 Dissipativity

For Eq. (3), we can obtain

$$\nabla V=\frac{\partial \dot{x}_1}{\partial x_1}+\frac{\partial \dot{x}_2}{\partial x_2}+\frac{\partial \dot{x}_3}{\partial x_3}=\begin{cases} -\beta\gamma-pb, |x_3|>1 \\ -\beta\gamma-pa, |x_3|\le 1 \end{cases} \quad (5)$$

Note that ($-\beta\gamma$ - pb) is a negative value. Thus the volume elements are contracting. After a time unit, this contraction reduces a volume V_0 by a factor $e^{-(\beta\gamma+pb)t} = e^{-127.10^{-4}t}$, which means that each volume containing the trajectory of this dynamical system converges to zero as $t\rightarrow\infty$ at exponential rate ($\beta\gamma$ + pb). Therefore, all system orbits are ultimately confined to a specific subset having zero volume and the asymptotic motion settles onto an attractor [32-37].

3.3 Poincaré Section

Poincaré sections can be an effective method to analyze the characteristics dynamic of nonlinear systems. According to nonlinear dynamics theory, the performance of the system can be judged by observing the number of the cutoff points on the Poincaré sections. One point or a few discrete points indicate that the converter is working in periodical state, while the cutoff point with a fractal structure reveals a chaotic behavior.

The Poincaré section is computed for $x_1 = 0$ when the frequency is 20 Hz. From Fig. 4, it can be seen that the symmetry is around the nominal voltage capacitor V_{cn} [38]. We also see a local symmetry around the floating capacitor voltages 0 and 100.

3.4 First Return Map

Another tool which illustrates the interesting dynamics

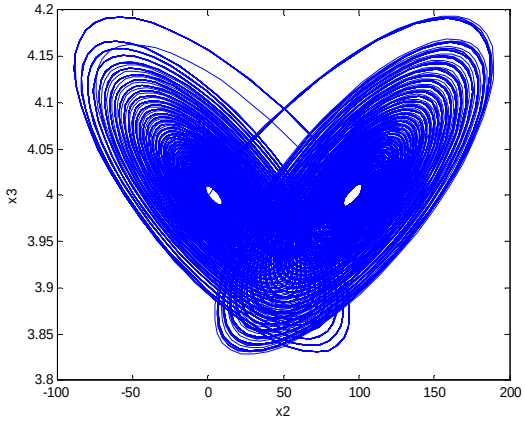

Fig. 4 Phase plane strange attractors x_3 versus x_2.

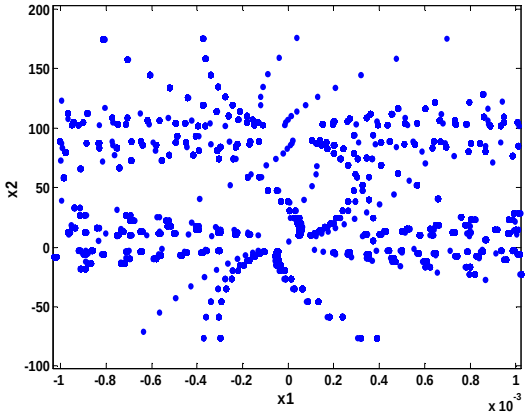

Fig. 5 The Poincaré section of x_1 versus x_2 plane.

of two cells chopper attractor is the Poincaré first return map. We again take a cross section of the band by cutting through it with a plane perpendicular to the flow (for our purposes the portion of the x_1 versus x_3 plane with $|x_1|<0.01$ works well). We then record the x_3 value of a trajectory when it crosses our plane

and graph it against the x_3 value of the next time the trajectory crosses the section. In this way, we can investigate the mixing which is done by the twist in the attractor.

From Fig. 5, it can be seen that there is a folding point at each end of the cross and obviously symmetry occurs [39].

3.5 Bifurcation Diagram

From Fig. 6, it can be seen that the system is chaotic for low frequencies. When the frequency becomes very large, the behavior of the system remains

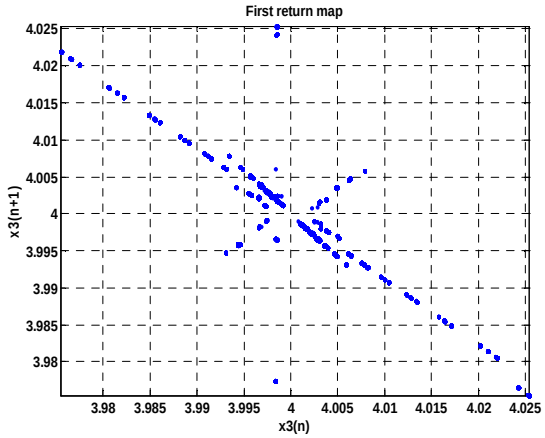

Fig. 6 First return map.

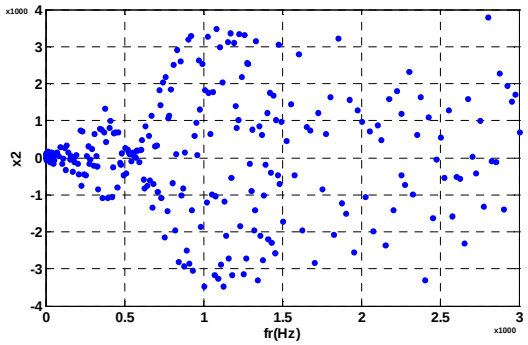

Fig. 7 Bifurcation diagram.

chaotic up to resonance and the load current reaches its maximum. When the switching frequency is higher than the resonance frequency $f_r = \frac{\sqrt{C + C_L}}{2\pi\sqrt{LCC_L}} = 2253.6\,\text{Hz}$, the system behavior changes from the strange attractor to an equilibrium point.

3.6 Spectrum Map

The power spectrum is also an effective way to analyze the stability of the circuit. When the circuit operates in the cycle, the peak of the waveform will only appear when the frequency is equal to times of the operating frequency (is a positive integer).

When the circuit in a chaotic state, the power spectrum manifesting as a continuous spectrum, which contains a peak corresponding to the periodic motion. The results are in good agreement with the previous analysis, which further verify the correctness of the results obtained by theoretical analysis.

The spectrum of this nonlinear system in Eq. (3) is also studied, its spectrum is continuous as shown in Fig. 7. It can be seen from Fig. 7 that the system exhibits chaotic behaviors.

4. Routes to Chaos

The initial values of the system are selected as (0, 5, 4). Using Simulink/Matlab the numerical simulation have been completed. This nonlinear system exhibits the complex and abundant chaotic dynamics behaviors, the strange attractors are shown in Fig. 8. These phase portrait are obtained by solving Eqs. (1)-(4) by means of Runge Kutta method for step size of 0.000001.

One of the routes to chaos observed in studied multicellular chopper is scroll doubling, which continues until there are no further stable states. At the beginning of simulation $u_1 = u_2 = 0$.

Now it is clear that the double scroll attractor has a structure quite different from the well-known Lorenz [40], Rössler [41] and Chua [42] attractors since the double-scroll structure has not been observed with the latter attractors.

When system parameter vary, periodic state becomes unstable because of period doubling scroll. Between 0.25 Hz and 20 Hz, one has a double scroll centered around the equilibrium points. From 25 Hz (Fig. 8d), the second scroll tends to disappear.

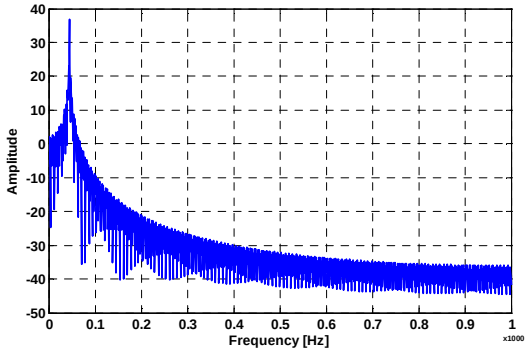

Fig. 8 Power spectrum of x_1.

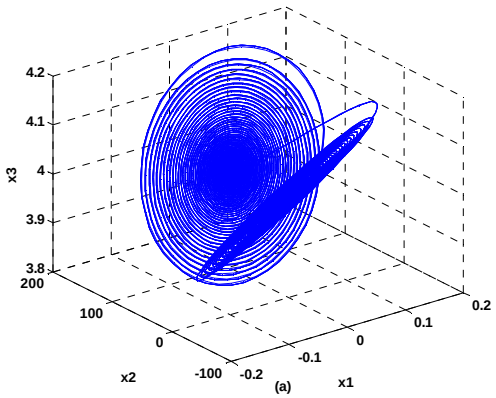

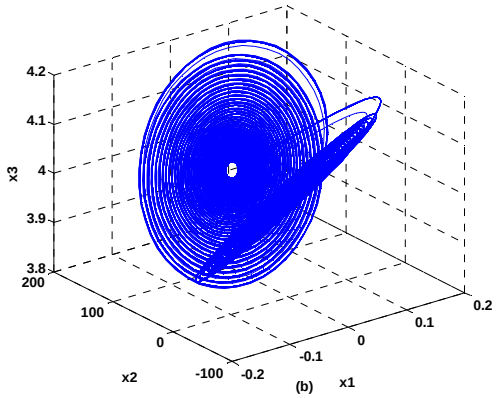

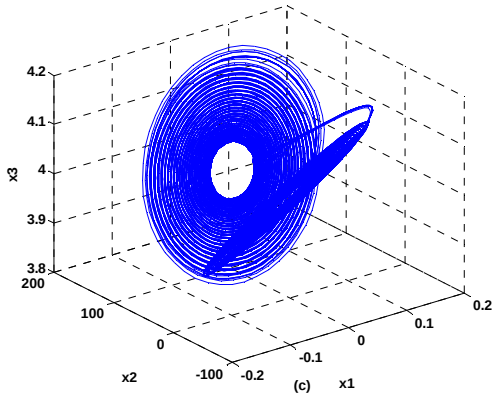

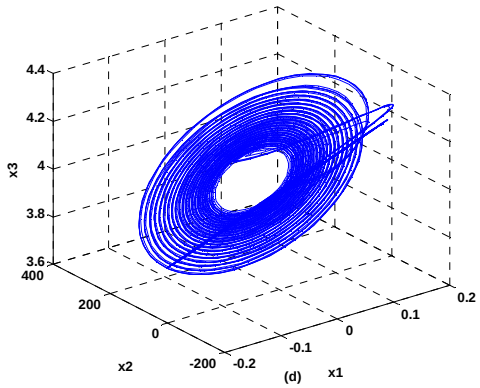

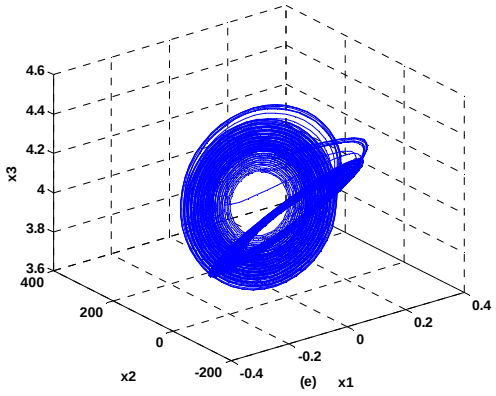

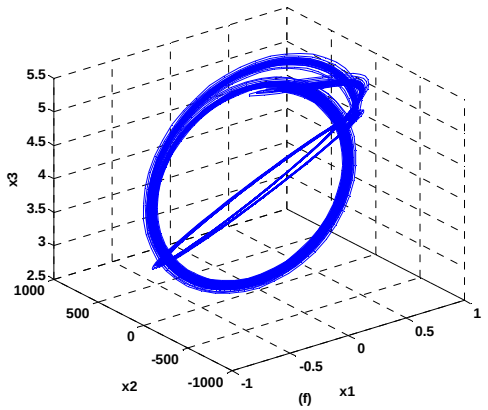

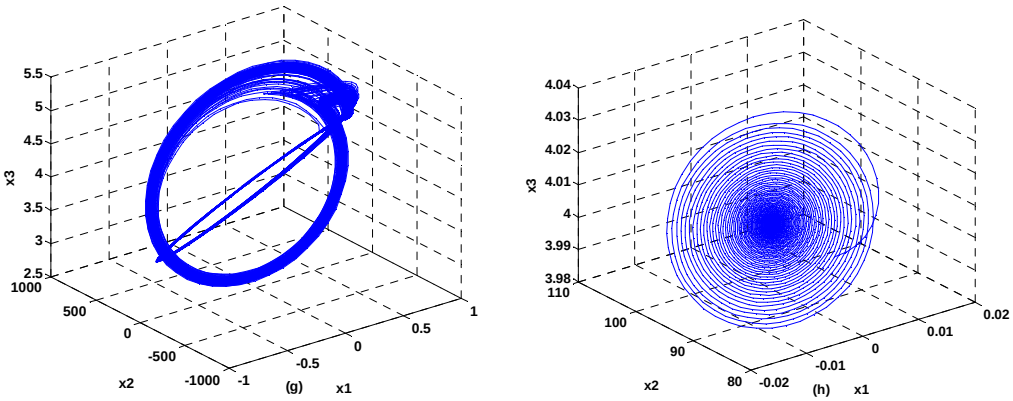

Fig. 9 Phase portraits: (a) fs = 1 Hz, (b) fs = 10 Hz, (c) fs = 20 Hz, (d) fs = 25 Hz, (e) fs = 50 Hz, (f) fs = 250 Hz, (g) fs = 500 Hz, (h) fs = 50 kHz.

When the switching frequency becomes large, we have a single scroll (Fig. 8h). For fs = 250 Hz and fs = 500 Hz, the attractor evolves into the limit cycles; the limit cycles are shown in Fig. 8f and Fig. 8g.

5. Conclusions

This note has presented the two cells chopper chaotic. These new attractors are different from the Lorenz attractor; Rössler and Chua, but it is a new butterfly shaped chaotic attractor. These new attractors need further study and exploration. Their topological structure should be completely and thoroughly investigated. It is expecting that more detailed theory analysis and simulation investigation will be provided in the near future. The dynamical behaviors of the two cells chopper associated to a particular nonlinear load are analyzed, both theoretically and numerically, including some basic dynamical properties, first return map, bifurcation diagram, Poincaré section, power spectrum and routes to chaos. As a result, they achieve the same results.

References

[1] Erickson, R., and Maksimovic. D. 2001. *Fundamentals of Power Electronics*. (2nd ed..)Dordrecht: The Netherlands: 576.

[2] Rodriguez, J., Lai, J. Sh., and Peng, F. Zh. 2002. "Multilevel Inverters: a Survey of Topologies, Controls, and Applications." *IEEE Trans. on Industrial Electronics*. 49 (4): 724–38.

[3] Meynard T. A., and Foch, H. 1998. Electronic Device for Electrical Energy Conversion between a Voltage Source and A Current Source by Means of Controllable Switching Cells. European Patent 92/916336.8, filed July 8, 1992, and issued April 7, 1998.

[4] Meynard, T. A., and Foch, H. 1992."Multilevel Choppers for High Voltage Applications." *European Power Electronics and Drives Journal.* 1(2): 4550.

[5] Meynard, T. A., Fadel, M. and Aouda N. 1997. "Modeling of Multilevel Converters." *IEEE Trans.Ind. Electronics*. 3 (44): 356-64.

[6] Robert, B., Abdelali El A., and Fadel, M.. 2005. "Modeling Discrete Time a Converter of Electrical Energy." In *Proceedings of 8th Meeting of the Nonlinear, Paris, France.*

[7] Bernardo, M. D., and Chi. K. T. 2002. "*Bifurcation and Chaos in Power Electronics: An Overview in Nonlinear Dynamics in Engineering*." Edited by Chen, G., New York: World Scientific 317-40.

[8] Defay, F., Llor, A. M., and Fadel. M. 2008. "A Predictive Control with Flying Capacitor Balancing of a Multicell Active Power Filter." *IEEE Trans. On Industrial Electronics* 55 (9): 3212–20.

[9] Ghanes, M., Trabelsi, M., Shi, X. L., Barbot, J. P., and Retif, J-M. 2012. "High Gain Observer Based on z(tn) Observability for a 3-Cell Chopper: Design and Experimental Results." *International Journal of Robust and Nonlinear Control* 24 (6): 1090-1103. ISSN 1049-8923

[10] Leon, J. I., Portillo, R., Vazquez, S. and Padilla, J. J. 2008. "Simple Unified Approach to Develop a Time-domain Modulation Strategy for Singlephase Multilevel Choppers." *IEEE Trans. on Industrial Electronics* 55 (9): 3239-48.

[11] Bernardo, M. D. and Chi, K. T. 2002. "Chaos in Power Electronics: An Overview." *Chaos in Circuits and*

Systems. New York: World Scientific 317-40.

[12] Yvon Ch. 1999. "Newsletter of the Laboratory of Electronics and Industrial Electronics." July 99 Number 1 www.thierry-lequeu.fr/data/LEEI-I1.pdf

[13] Tse, C. K., *Complex Behavior of Switching Power Converter*. CRC Press, 2003.

[14] Barbot, J. P., Saadaoui, H., Djemaı, M., and Manamanni, N. 2007. "Nonlinear Observer for Autonomous Switching Systems with Jumps." *Nonlinear Analysis: Hybrid Systems* 1 (4) 537-47.

[15] Benmansour, K., Tlemani, A., Djemaı M., and De Leon J. 2010. "A New Interconnected Observer Design in Power Converter: Theory and Experimentation." *Nonlinear Dynamics and Systems Theory* 10 (3): 211-24.

[16] Contopoulos, G. 2002. *Order and Chaos in Dynamical Astronomy*. Berlin: Springer Verlag.

[17] Benettin, G., Galgani, L., and Strelcyn, J. M. 1976. "Kolmogorov Entropy and Numerical Experiments." *Phys. Rev*. A14: 2338-445.

[18] Froeschlé, C., Lega, E., and Gonczi, R. 1997. "Fast Lyapunov Indicators. Applications to Asteroidal Motion." *Celest. Mech. Dyn. Astron* 67: 41-62.

[19] Skokos, C. 2001. Alignment Indices: A New, Simple Method for Determining the Ordered or Chaotic Nature of Orbits." *J. Phys.* A34: 10029-43.

[20] Skokos, C., Bountis, T. and Antonopoulos, C. 2007. Geometrical Properties of Local Dynamics in Hamiltonian Systems: The Generalized Alignment Index (GALI) Method." *Physica D*: Physica D: Nonlinear Phenomena, 231 (1): 30–54

[21] Binney, J., and Spergel, D. 1982. "Spectral Stellar Dynamics." *Astrophys. J*. 252 (1): 308-21

[22] Laskar, J. 1990. "The Chaotic Motion of the Solar System: A Numerical Estimate of the Size of the Chaotic Zones." *ICARUS* 88(2): 266-91.

[23] Gottwald, G. A., and Melbourne, I.2004. "A New Test for Chaos in Deterministic Systems." *Proc. R. Soc. Lord*. A 460 (2042): 603-11.

[24] Horwitz, L., Zion, Y. B., Lewkowicz, M., Schiffer, M., and Levitan, J. 2007, "Geometry of Hamiltonian Chaos." Phys Rev Lett. 98(23):234-301

[25] Wu, X. 2009. Is the Hamiltonian Geometrical Criterion for Chaos Always Reliable?." *Journal of Geometry and Physics*.59(10) 1357-62

[26] Levin, J. 2000. "Gravity Waves, Chaos, and Spinning Compact Binaries." *Phys. Rev. Lett* 84: 3515.

[27] Davaucens, P. and Meynard, T. 1997. Study of Parallel Multicell Converters: Analysis of the model *J. Phys. III France*.7 (1): 161-77.

[28] Gateau, G., Maussion, P., and Meynard. T. 1997. "Modeling the nonlinear control of serial multicellular converters: Application to the chopper function". *J. Phys. III France*. 7 (6): 1277-305.

[29] Meynard T. A., and Foch. H. Device for conversion of electrical energy to semiconductor. French Patent, 91,09582, Europe, Japan, USA, Canada, 92,00652.

[30] Benmansour, K., Leon, J. D., and Djemai. M. 2006. "Adaptive Observer for Multi-cell Chopper." In *Proceedings of Second International Symposium on Communications, Control and Signal Processing*, Marakesh, Morocco.

[31] Gateau, G., Fadel, M., Maussion, P., Bensaid, R., and Meynard. T. A. 2001. "Multicell Converters: Active Control and Observation of Flying-capacitor Voltages." *IEEE Trans.Ind. Electronics* 49 (5): 998–1008.

[32] Wei, Z., and Yang, Q. 2011."Dynamical Analysis of a New Autonomous 3-D Chaotic System Only with Stable Equilibria." *Nonlinear Anal.: RWA*. 12 (1): 106-118.

[33] Dadras, S., and Momeni, H. R. 2009. "A Novel Three-Dimensional Autonomous Chaotic System Generating Two, Three and Four-scroll Attractors." *Phys. Lett. A*. 373(40): 3637-42.

[34] Zhou, W., Xu, Y., Lu, H., and Pan, L. 2008. "On Dynamics Analysis of a New Chaotic Attractor." *Phys. Lett. A*. 372 (36): 5773-7.

[35] Li, X. F., Chlouverakis, K. E., and Xu, D. L. 2009. "Nonlinear Dynamics and Circuit Realization of a New Chaotic Flow: A variant of Lorenz, Chen and Lü." *Nonlinear Analysis: Real World Applications* 10 (4): 2357- 68.

[36] Yu, F., and Wang, C. 2012. "A Novel Three Dimension Autonomous Chaotic System with a Quadratic Exponential Nonlinear Term." *Eng. Technol. Appl. Sci. Res.* 2(2): 209-15.

[37] H. Dang-Vu, and C. Delcarte. 2000. Bifurcation and Chaos: An Introduction to the Contemporary Dynamics with Programs in Pascal, Fortran and Mathematica, (Ellipses, Paris).

[38] Gilmore, R. and Letellier, C. 2007. *The Symmetry of Chaos*. USA: Oxford University Press.

[39] Djondiné, P., He, R., Ghanes, M., and Barbot, J. P. 2013. "Chaotic Behavior Study for Serial Multicellular Chopper Connected to Nonlinear Load." In *Proceedings of the 3rd International Conference on Systems and Control*. Algiers, Algeria.

[40] Lorenz, E. N. 1963. "Deterministic no Periodic Flow." Journal of the Atmospheric Sciences, 20(2): 130-41

[41] Rössler, E. 1976. "An Equation for Continuous Chaos." Physics Letters A 57 (5): 397–98

[42] Chua, L. O. 1994. "Chua's Circuit: An Overview Ten Years Later." *Journal of Circuits, Systems and Computers* 4 (2) 117-59.